Numerical Simulation of Polar Lows and Comma Clouds Using Simple Dry Models*

STEPHEN E. MUDRICK

Department of Atmospheric Science, University of Missouri—Columbia, MO 65211

(Manuscript received 25 August 1986, in final form 20 April 1987)

ABSTRACT

Linear and nonlinear numerical channel models are used to simulate polar low/comma cloud evolution. The purpose of this study is to see how much realism can be obtained using models that do not include water vapor. The study was inspired by several observations of such features that evolved over North America.

The basic state used is zonally independent, with an east–west oriented polar front jet on a beta plane centered at 60°N latitude. Strong horizontal as well as vertical wind shear is present. The lowest 3 km of the channel has a reduced static stability, simulating the effect of destabilization from below by sensible heat fluxes upon the polar air mass. The models contain 10 vertical levels.

The linear results are consistent with earlier studies. The most unstable normal modes given by the linear, quasi-geostrophic model show growth rates increasing as the zonal wavelength decreases down to 700 km, the shortest wavelength for which the model gives meteorologically meaningful results. The mechanism of growth is baroclinic instability. The enhanced growth rates at short wavelengths are due to the presence of the layer of reduced stability. Growth rates for wavelengths similar to the scales of polar low/comma clouds, $\sim 10^3$ km, are as large as observed cases. These short wavelength normal modes are quite shallow, in contrast to some observed polar low/comma cloud cases.

Three-dimensional, fully nonlinear, dry, quasi-geostrophic and primitive equations models are then used to study the evolution of a 1200 km wavelength normal mode superimposed upon the basic state. Results of a "fine-resolution" primitive equations run (Δx, $\Delta y = 50$ km) are emphasized. The disturbance undergoes a rapid life cycle lasting ~3 days and deepens somewhat at midtropospheric levels, in contrast to the linear and nonlinear quasi-geostrophic cases. At the channel bottom a cyclonic vortex ~500 km across forms, associated with a broad, weak ridge but no closed contour high. An elongated cold front and a short warm front form by day 1. The frontal configuration can be interpreted alternatively as a cold front with an occluded region nearest the low center. All these features are similar to observed polar low/comma cloud cases, both on the disturbance scale and on the frontal scale.

The results appear realistic in many ways and suggest that dry baroclinic instability, operating upon regions of reduced static stability in the lower troposphere, can explain the initial stages of polar low/comma cloud development.

1. Introduction

Polar lows or polar troughs, and related features, "comma clouds," are subsynoptic-scale disturbances that form under the cyclonic side of the polar front jet or further back in the cold-air outflow. They can move fairly quickly and have rather small horizontal dimensions, on the order of 10^3 km. They can develop quite rapidly and may become quite intense. Over the northern oceans they seem to be associated with large fluxes of sensible heat from the surface and with latent heat release, often in convective form, but sometimes they are observed over land with little precipitation. The work described herein was inspired by such "land" cases, in particular the Mullen (1982) study.

In this paper we shall refer to such features as "polar low/comma clouds" (PL/CC). Good introductory reviews of these features are given by Reed (1979), Rasmussen (1983) and Sardie and Warner (1983). Two themes run through the work concerning this subject. An observational study by Harrold and Browning (1969) concluded that a polar low crossing England was a short-wavelength, baroclinic feature. Theoretical work by Mansfield (1974), Duncan (1977), Staley and Gall (1977) and by Blumen (1979) supports that conclusion, indicating that large lapse rates and strong vertical wind shear at low levels leads to short-wavelength baroclinic wave growth.

On the other hand, the importance of latent heat release, conditional instability of the second kind (CISK) in particular, as the major energy source for such disturbances has been stressed by Rasmussen (see his 1983 paper) and others. Reed (1979) studied North Pacific comma clouds and concluded that CISK was probably of secondary importance in their development, compared to baroclinic instability effects. Some authors have concluded that CISK processes may be of more importance for Atlantic polar lows than for

* Contribution from the Missouri Agricultural Experiment Station, Journal Series No. 10153.

Pacific comma clouds (Locatelli et al., 1982; Sardie and Warner, 1983).

Discrepancies between the linear, dry studies and observed results, particularly the shallow nature of the solutions compared to the often deep structure of observed cases (Reed, 1979) has led to most theoretical work proceeding in the direction of adding moisture dynamics to the models to enhance realism (e.g., Sardie and Warner, 1983). Little work has been done on pursuing the dry models beyond the linear, quasi-geostrophic stage in order to see how realistically these models can simulate PL/CC. More can be done. Reed (1979) points out that the use of zonally independent basic states, often lacking horizontal shear, is too simplified. Blumen (1980) provides an explanation of how a dry model can be reconciled with deep disturbances. His two-dimensional model involves the nonlinear interaction of shallow and deep waves. Orlanski (1986), using a two-dimensional, dry model, studies the role of surface sensible heat fluxes in the nonlinear evolution of subsynoptic-scale waves. He shows that growth rates can be greatly increased by the addition of localized regions of enhanced surface heat fluxes, but it does take the addition of moisture to allow the shallow wave to become "deep", in agreement with the results of Gall (1976).

A recent paper by Kent Moore and Peltier (1987), using a dry, frictionless, semigeostrophic, linear model, studies the instability of Hoskins and Bretherton (1972) frontal zones. They find unstable disturbances with wavelengths of $\sim$1000 km which grow via baroclinic instability. They argue that their analysis applies to PL/CC initiation as well as to frontal cyclones. Their disturbances are quite shallow, similar to the results of quasi-geostrophic linear studies.

This paper will deal with the following question: How far can dry models go toward producing realistic PL/CC simulations? This will shed light on whether moisture is of primary or of secondary importance in the early development of such phenomena. Certainly moisture is of major importance in the mature, deep oceanic disturbances, but examples of polar lowlike phenomena have been observed over land where moisture is probably of secondary importance (Wallace and Hobbs, 1977, pp 112 and 122; Mullen, 1982; Smart and Carr, 1986). While regions of enhanced convection often precede the development of PL/CC as Reed (1979, section 2) points out for Pacific cases, the process that allows the disturbed regions to reach finite amplitude could be the "dry" baroclinic instability as opposed to CISK processes.

In addition, recent studies suggest a further look at nonlinear, three-dimensional, nonquasi-geostrophic, dry model simulations may be in order. Sardie and Warner (1985) use a "state of the art" mesoscale model to attempt to forecast an observed Atlantic polar low evolution. The "dry run" without latent heat feedbacks forecasts the 48-h location of the low, albeit too weakly, in approximately the correct location. Orlanski (1986), in his introduction, mentions apparently similar simulations: "A surprising feature of these studies is that weak [subsynoptic-scale] cyclones develop for the dry simulations in approximately the same geographical position as those simulations having latent heat release; this suggests that the dry atmosphere may have the necessary ingredients for the development of [subsynoptic-scale] cyclones, and that latent heat makes its development explosive."

Thus it seems reasonable to simulate the evolution of PL/CCs using a dry, primitive equations nonlinear model with three dimensions and with enough gridpoints to resolve features with wavelengths on the order of 10^3 km. This paper will present such results. The models used here, a linear and a nonlinear quasi-geostrophic model as well as the primitive equations model, will deliberately be quite simple. They are adiabatic, except for a surface drag form of friction in the primitive equations model and are described in section 2. The basic state is quite idealized and can be specified analytically. It possesses strong horizontal as well as vertical wind shear and implicitly includes the effect of sensible heat fluxes from the lower boundary. This is done by having a layer of reduced stability present in the lower troposphere, as described in section 3. The results of the linear model study are presented in section 4; these are used to provide input for the nonlinear model integrations discussed in section 5. We will see that, given sufficient horizontal resolution, many features of PL/CC can be simulated by the nonlinear primitive equations model and the idealized basic state, and in particular, a rapidly growing disturbance with a wavelength on the order of 10^3 km.

2. Description of the models used

The models used here are restricted to dry, hydrostatic, adiabatic motion. The Boussinesq approximation is made. The flow is assumed to be inviscid, except for the addition of a short-wave filter and surface drag, which is present in some of the runs. The atmosphere is simulated by an east–west reentrant channel with rigid horizontal and vertical boundaries, located on a beta plane. The artificial effect of the walls is minimized by selecting initial conditions such that nothing happens near the walls. No topography is present.

The two-dimensional, linear, frictionless, quasi-geostrophic model (2DINIT) is described in section 2 of Mudrick (1979). This model is really three-dimensional in that the zonal perturbation structure is assumed to be that of a normal mode, i.e., sinusoidal.

The fully three-dimensional, nonlinear primitive equations (PE) and quasi-geostrophic (QG) models are described and referenced in Mudrick (1982, hereafter known as M). Surface friction has been added to the lowest level only of the PE model by using a drag coefficient approach. The terms added to the x and y mo-

mentum equations are proportional to $-K|V_1|u_1$, $-KV_1v_1$ where u_1, v_1 are the x and y velocity components at the lowest level in the model, $|V_1| = (u_1^2 + v_1^2)^{1/2}$ and $K = 1.5 \times 10^{-3}$. No diffusion term has been added to the adiabatic thermodynamic equation. The third-order, "INT" form of horizontal filter is used for the PE and QG models, as described in M, p 2420.

For all integrations, with all models, 10 levels in the vertical are used. The "coarse resolution" runs have Δx, $\Delta y = 100$ km with a channel length of 1200 km and width of 3600 km; these coarse runs require 14 $\times$ 38 $\times$ 10 points for each variable. The "fine-resolution" PE run uses Δx, $\Delta y = 50$ km. The channel width is reduced from 3600 to 2400 km; no problems developed near the walls during this integration. Still, 26 $\times$ 50 $\times$ 10 points are required for each variable and the timestep is reduced from 4 to 2½ min for the fine-resolution run.

3. The initial state

This section describes the zonally independent basic state used for the linear growth rate study and the procedure for determining the initial states which are used for the nonlinear integrations.

a. The basic state

The zonally independent basic state used to model the region within which PL/CC develop is similar in structure to the basic states desribed in M, section 4 (see especially Fig. 1 and Table 1). The major difference, as discussed below, is the addition of a region of reduced stability in the lowest 3 km of the troposphere. This reduced stability models the effect of destabilization from below as the cold air moves equatorward across the land or ocean surface. It is within these cold air outflows that PL/CC tend to form.

For the lowest layer, a temperature lapse rate of 9.0°C km^{-1} is used, while the lapse rate for the remainder of the troposphere is 6.6°C km^{-1}. The stratospheric lapse rate is -2.0°C km^{-1}, i.e., the temperature increases with height. These lapse rates, along with an assumed temperature of 246 K at 5 km ($\sim$540 mb), as idealized from Mullen (1979, Fig. 2 and 1982, Fig. 7), define the meridionally averaged vertical temperature profile. A temperature increase is used in the lower stratosphere, rather than isothermal conditions as in M, because otherwise the 2DINIT model used to deduce the normal-mode structure, as described below, does not converge to meteorologically realistic solutions.

Other parameters describing the basic state characteristics are as follows (these can be compared to corresponding values for basic states used in M; see Fig. 1 and Table 1 in M): channel depth $H = 15$ km, width $D = 3600$ km, $f_0 = 1.25 \times 10^{-4}$ s^{-1} (corresponding to 60°N), $U_0 = 0$ m s^{-1}, $U_M = 75$ m s^{-1}, $U_T = 56$ m s^{-1}, D_J the jet width = 2000 km, $Y_J = 2133$ km (the jet is skewed toward the cyclonic side in order to keep the absolute vorticity positive) and the meridional temperature change in the lower troposphere is 27°C.

Thus the idealized basic state uses a rather strong jet (max = 75 m s^{-1}) in a channel centered at 60°N, with a region of reduced stability in the lowest 3 km; these are the three major departures from earlier basic states used in M. As in M, the basic state used here is barotropically as well as baroclinically unstable.

The use of these three features for modifying the basic state are justified from other model and observed studies of PL/CC development. Diverse results from various papers suggest the values used here are not unreasonable. Duncan (1977) presents data (his Table 3) suggesting the presence of the top of a layer of reduced stability (LRS) at between 800 and 700 mb for three cases he studied. Blumen (1980) refers to Duncan's paper as justification for his LRS of 2–4 km in depth. Harrold and Browning's (1969) LRS is 2–6 km in depth. These are all "Atlantic" cases; Mullen (1979, Fig. 6B, p 1644) has the top of a LRS anywhere from 850 to 700 mb, i.e., $\sim$1.5 to 3 km in depth, for his North Pacific study.

Thus, the depth of 3 km seems reasonable in this study. To a great extent this depth was required, given the limited vertical grid resolution of 1.5 km (10 levels in a depth of 15 km). It was desired that the LRS contain at least two grid points within it, requiring a depth of 3 km. (A layer of only 1.5 km in depth, containing one gridpoint, also was used; the dotted curve in Fig. 1 shows results for the linear study similar to those using the 3 km LRS.)

With respect to the value of the lapse rates used, there is some evidence that lapse rates approaching dry adiabatic may be found in the lower troposphere for these situations. Harrold and Browning (1969, Fig. 8B, p 719) show a nearly dry adiabatic layer extending upward to 800 mb in the region of a developing oceanic polar low. This is occurring with light surface winds, as in our basic state. Forbes and Lottes (1985, p 145) find lapse rates for the 1000–850 layer averaging 8.1°C km^{-1} for a study of North Atlantic vortices during an anomalously cold month (Dec. 1981). Mullen's (1979) N. Pacific data (Fig. 6b) show conditionally unstable lapse rates in the lower troposphere. Orlanski (1986, p 2) discusses a mid-Pacific comma cloud simulation which utilizes a region "of very weak static stability" from the surface up to about 750 mb, i.e., $\sim$2.5 km. These separate cases suggest that a value of 9°C km^{-1} is not unreasonable for the lapse rate in the LRS.

Likewise, a value of 6.6°C km^{-1} for the midtropospheric lapse rate is similar to values of 6.9 and 6.2 deduced from profiles B and C, respectively, from Mullen (1979, Fig. 6B), for the lapse rate from 700 to 400 mb. Forbes and Lottes (1985) report the average lapse rate to be about 7°C km^{-1} for the region from 850 to 500 mb for their case study.

While a maximum speed of 75 m s^{-1} is large, the vertical wind shear beneath the jet core of 75 m s^{-1}/10 km or 7.5×10^{-3} s^{-1} is similar to the average value

of 7×10^{-3} s^{-1} for the 1000–300 mb layer found by Mullen (1979, Fig. 3B) for the "genesis stage." It is realized, however, that not all PL/CC develop in a region of such enhanced vertical wind shear and such deep baroclinicity. Mansfield (1974) and Forbes and Lottes (1985) study Atlantic situations where fairly weak upper-tropospheric vertical shear is present. Our basic state is more similar, perhaps, to Mullen's North Pacific study but some features in common with North Atlantic cases were also previously noted.

Polar lows are found anywhere from, say, 40° and poleward to 65° and beyond (Rasmussen, 1983). For this study a latitude of 60° was used for the channel. This is the value used by Duncan's (1977) *f*-plane channel model study. While Mullen's (1979) North Pacific cases are near 40°N, his "land polar low" case (1982) is closer to 60°N. The North Atlantic cases tend to be further north than are the North Pacific cases.

b. The initial conditions for the models

With the basic state given, the linear study was carried out using the 2DINIT model. A particular channel length was chosen and the most rapidly growing normal mode for that wave length was found, as discussed in section 4. In order to integrate the nonlinear, three-dimensional PE and QG models, the initial state was obtained by superimposing the normal-mode perturbation appropriate for the particular channel length onto the basic state. The perturbation magnitude was chosen to be small so that initially the growth would be of a linear nature. For the QG model, this superposition gave the total streamfunction, which is the initial pressure field. For the PE model, small corrections were added for the initial wind and buoyancy fields, based on the next higher-order terms in the Rossby expansion used in deriving the quasi-geostrophic theory. The resulting initial pressure field for the PE model was thus slightly different than the QG initial pressure field. Section 5 provides details of the nonlinear integrations.

4. The linear results**

A linear study of the instability of the basic state was first undertaken using the 2DINIT model previously discussed. The following procedure was used. A particular channel length was chosen; this defined the zonal wavelength of the normal mode solution. The 2DINIT integration was then initiated by introducing a small perturbation and the run was terminated when the solution had converged to the fastest-growing normal mode. The 2DINIT model gives the growth rate and propagation speed as well as the structure of the normal mode for the channel length, i.e., wavelength chosen. Another channel length was then chosen and the procedure was repeated. See Mudrick (1979) for details.

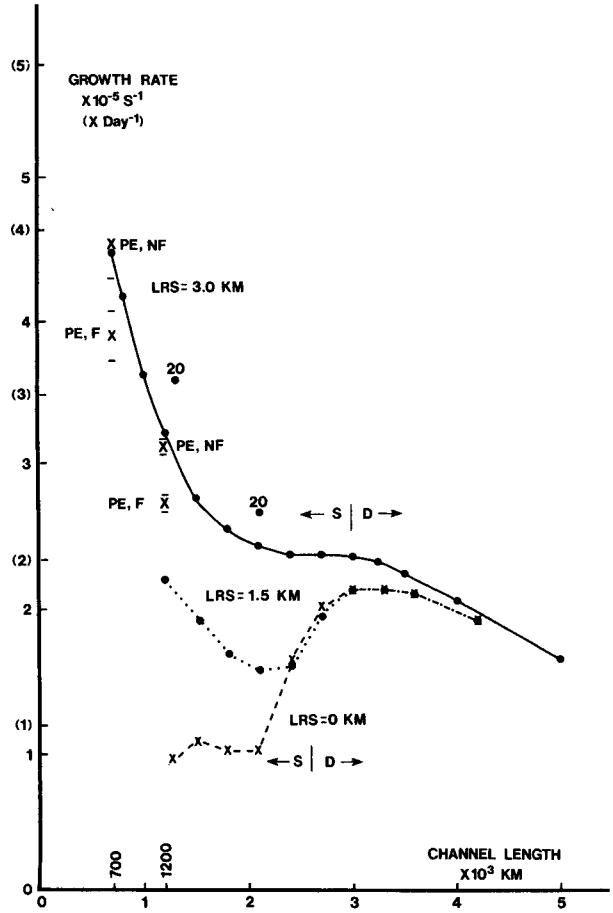

FIG. 1. Instability results for basic states possessing layer of reduced stability (LRS) of: 3 km (solid), 1.5 km (dotted) and 0 km (dashed). Growth rate $\times 10^{-5}$ s^{-1} (and day^{-1} in parentheses) versus channel length $\times 10^3$ km. See text for details.

Figure 1 presents growth rates, in days^{-1} and s^{-1}, plotted against channel length (wavelength) in km. The curves are for the basic state with (solid) and without (dashed) the layer of reduced stability in the lowest 3 km. In other words, the basic state tropospheric temperature lapse rate was 6.6°C km^{-1} for the entire troposphere, for data on the dashed curve. The "S" and "D" indicate that the maximum disturbance amplitude, averaged over the channel length, is at the lowest level in the channel (shallow) or at jet-core level (deep), respectively. Thus, modes with wavelengths <2500 km are shallow disturbances, as discussed below.

Results to be emphasized are the following:

1) The presence of the LRS in the lower troposphere is seen to be responsible for enhanced growth rates for wavelengths <3000 km (compare solid and dashed curves).

2) Growth rates are quite large in the vicinity of 10^3 km, the horizontal scale of PL/CC (500–1500 km). For 1200 km the doubling time is 0.25 days.

** *Note added in proof:* Staley et al. (1987) discuss results—many similar to those presented here—using a multilevel, linear, quasi-geostrophic model.

3) The growth rate increases with decreasing wavelength, to 700 km. Below 700 km 2DINIT converges to a nonmeteorological mode so the results in Fig. 1 cannot be extended to shorter wavelengths. Thus, *no wavelength of maximum instability is found.*

4) Modes with horizontal scales similar to those of PL/CC (<1500 km) are quite shallow.

5) The barotropic instability mechanism is not important, compared to baroclinic instability.

The remainder of this section will involve the elaboration of the above points. First, however, one may argue that given the strong shear and short wavelengths used here, the quasi-geostrophic approximation may be of limited validity. One justification for using it is that the results obtained here can then be compared to other quasi-geostrophic studies of PL/CC. This will be done presently.

A second, a posteriori justification is provided by the comparison of growth rates from the three-dimensional, nonfriction PE model runs with the 2DINIT results. This was done for channel lengths of 700 and 1200 km. The normal modes given by 2DINIT were superimposed with a small initial amplitude upon the basic state and the resulting initial states were integrated in time in the PE model, as previously explained. The growth of channel-integrated eddy kinetic energy was used to determine PE growth rates during the linear phase of growth. These values are indicated by "PE, NF" values as Fig. 1. The error bars indicate the uncertainty in the slope of the line drawn on semilog paper used for plotting the eddy kinetic energy versus time. The PE values are seen to be consistent with the linear QG analysis. The same limited vertical resolution of 10 levels and the same horizontal resolution was used for the PE runs as was used for 2DINIT. A detailed comparison of the 2DINIT and PE linear phase perturbation structure was not made.

Additional comments concerning these points follow, i.e., point 1) following corresponds to 1) previously mentioned, etc.:

1) The major result of the linear study is the presence of the enhanced growth rates for short wavelength disturbances due to the presence of the layer of reduced stability at the bottom of the channel. This suggests that the inclusion of large sensible heat fluxes from the underlying water or land surface, albeit included implicitly in this study, is needed for the development of rapidly growing baroclinic disturbances on the scale of PL/CC[1]. Comments that follow, concerning the results of Kent Moore and Peltier (1986), corroborate this. Linear studies of PL/CC development that include moisture dynamics have also included the effect of sensible heat fluxes, e.g., Sardie and Warner (1983) and Rasmussen (1983). The latter stresses the increased importance of the sensible heat flux in extratropical CISK systems compared to tropical ones. The Sardie and Warner (1985) nonlinear study concludes that even with moisture dynamics, the sensible heat flux is of great importance. Thus it seems that for any study that hopes to simulate PL/CC disturbances, inclusion of the sensible heat flux is required.

2) A comparison of Fig. 1 presented here and Table 3 of Sardie and Warner (1983), giving growth rates deduced for six observed PL/CC cases, shows the frictionless 2DINIT growth rates to be as large as or larger than all observed cases. Even rescaling the growth rates for a 40°N channel, which means reducing the rates by 20%, still gives values larger than most of the above cases. While a direct comparison between the highly idealized basic state used here and the observed cases probably would be meaningless, we see at least that a QG model using dry baroclinic instability alone can give growth rates as large as those observed with some PL/CC cases.

This result is in contrast to the dry (BCD) model results of Sardie and Warner (1983), who used a three-layer QG model with the basic-state wind constant within each layer. As pointed out by Staley and Gall (1977) at least four layers and probably more are needed to describe accurately the instability of short-wavelength features (p 1680). In addition, the combination of strong horizontal and vertical wind shear plus reduced lower-tropospheric stability apparently allow for the greater growth rates for dry baroclinic instability found here. Earlier studies have noted the sensitivity of growth rates to static stability and to vertical wind shear, see, for example, Staley and Gall (1977), many of whose results are similar to those found here. In particular, Staley and Gall suggest that reduced lower-tropospheric stability and increased vertical wind shear both contribute to large growth rates at shorter wavelengths.

As an aside at this point, it should be noted that the large growth rates for short wavelengths shown in Fig. 1 correspond to deepening rates comparable to some of the "bomb" cases studied by Sanders and Gyakum (1980). Indeed, the integration using the dry, frictionless, three-dimensional, nonlinear QG model, for a 1200 km channel length, produced deepening rates greater than 1 mb h^{-1} for a 1 day period between days 0.7 and 1.7, just qualifying as a Sanders–Gyakum "bomb." Admittedly, the addition of surface friction would reduce the deepening rate somewhat, but it is seen that a QG model employing dry baroclinic instability can produce deepening rates significantly greater than suggested by earlier QG studies (e.g., Sanders and Gyakum, 1980) provided strong horizontal and vertical wind and temperature gradients are included in the model. To reiterate: apparently, the diabatic effect of the upward heat fluxes from the lower surface, which Sanders and Gyakum feel is needed in numerical models in order to achieve realistic deepening rates, is

[1] Disturbances could also be forced by midtropospheric developments, a situation not considered here but subsequently discussed.

contained indirectly in the dry model by including the layer of reduced stability in the basic state.

3) A discussion of the details of the curve in Fig. 1 and the question of where (or if) a wavelength of maximum instability exists will not be pursued further, beyond the following comments. Since the normal modes become more shallow and somewhat more narrow as the wavelength decreases, it is probable that the limited vertical resolution of ten levels and to the same extent the limited horizontal resolution of 100 km may cause significant error and hence the growth-rate curve may become increasingly inaccurate with decreasing wavelength. The lack of a wavelength of maximum instability above 700 km may thus be an artifice of the limited resolution.

James and Hoskins (1985, p 2147), examining the Eady baroclinic instability problem on a sphere, state that, to some extent, coarse vertical resolution was responsible for the large growth rates they found for very shallow, short-wavelength normal modes. On the other hand, 2DINIT was rerun with 20 levels in the vertical and with the same N–S resolution for 1300 km and 2100 km; the growth rates are shown in Fig. 1 as "20". These rates are even greater than the 10-level results and suggest the shape of the growth-rate curve is not in significant error due to the 10-level resolution, at least down to 1300 km.

The exact shape of the curve is also sensitive to the details of the shape of the basic-state jet, as well as to the details of the static stability profile, as other studies have shown (e.g. Duncan, 1977; Blumen, 1979; as well as Staley and Gall, 1977). Since the basic state chosen is only meant to be a simplified idealization of the atmospheric region within which PL/CC develop, there seems to be no need to further pursue the precise shape of the growth-rate curve.

One might expect that, since the short-wavelength disturbances are quite shallow, a major decrease in the growth-rate curve would occur if surface friction were included. To test this, surface friction was added to the lowest level of the PE model, as described in section 2, and the 700 and 1200 km PE runs were repeated. The linear phase growth rates are shown in Fig. 1 by the "PE, F" values. Adding friction is seen to reduce the growth rates, with the 700 km growth rate being reduced more than the 1200 km growth rate. Yet even with friction, the 700 km growth rate is greater than the 1200 km growth rate and no wavelength of maximum instability is found above 700 km.

This study includes the presence of a layer of reduced stability with a steep lapse rate but the absence of anything more than surface friction in the PE model (as described in section 2), and no friction in the linear QG model. It can be argued that since the layer of reduced stability is a region of enhanced vertical mixing and turbulence, the turbulence should be modeled by subgrid-scale mixing effects in the momentum equations. In other words, the results presented so far are biased if no representation of turbulent mixing is included in the models. Therefore, additional integrations were made with a "full friction" form of the PE model (see the Appendix). A zonal wavelength of 1400 km was used, and only results for the linear phase of growth were examined. The linear phase growth rate was 2.40 $\pm$ 0.07 $\times$ 10^{-5} s^{-1} compared to the no friction value of 2.80 $\times$ 10^{-5} s^{-1} (which can be deduced from Fig. 1). Thus, a reduction of about 14% in the growth rate of the 1400 km perturbation is caused by including the subgrid-scale turbulence, as opposed to a reduction of about 5% for a 1400 km integration with only the surface friction. The "full friction" growth rate is still over 2 $\times$ 10^{-5} s^{-1} which is quite large, suggesting the results presented here and in section 5 would not be changed in a major way even if the full-friction PE model had been used.

4) A major discrepancy of linear theory is that the waves are shallow, while PL/CC can be deep (Reed, 1979). Figure 2a shows the zonally averaged disturbance amplitude $(\overline{p'^2})^{1/2}$, where p' is the deviation from the zonally averaged p, for the 1200 km wavelength fine-resolution PE run at the start. This is virtually identical to the amplitude of the linear normal mode solution, and will be considered as such here. The maximum value is seen to be located under the polar side of the jet, similar to observed cases discussed by Reed (1979). The structure is seen to be quite shallow. The 1200 km result is typical of all wavelengths <1500 km. With decreasing wavelength, the modes become more shallow and of smaller meridional scale (and errors associated with the limited horizontal and vertical finite-difference resolution thus probably become larger, as previously discussed).

Orlanski (1986) derives an expression for the vertical scale for the kinetic energy of the waves. This "penetration depth" $\delta \sim C_r/(2d\bar{U}/dz)$ can be used to estimate the depth of the solutions found. For the 1200 km case, $C_r \sim 15$ m s^1, $d\bar{U}/dz = 7.5$ m s^{-1} km^{-1} so $\delta = 1$ km. This is consistent with Fig. 2a.

Forbes and Lottes (1985, p 152) point out that the quasi-geostrophic, linear models of Sardie and Warner (1983), among others, predict short wavelength development of shallow disturbances being favored by large low-level lapse rates and by large low-level vertical wind shear, as well as by weaker upper-level wind shear. Our basic state possesses strong upper-level wind shear but the quite shallow nature of our disturbances may mean the effect of the upper-level wind shear is minimal on the disturbances.

One way to reduce this discrepancy of shallow versus deep disturbances, as discussed in the Introduction, is to add moisture dynamics. Gall (1976), for example, showed that latent heat release caused short waves to possess a deeper structure than in dry models. The dry short waves were shallow, as are ours. Gall's moist model utilized a completely saturated atmosphere; using more realistic amounts of moisture may reduce the depth of the wave structure. It is clearly seen, however, that adding moisture deepens short-wave structure.

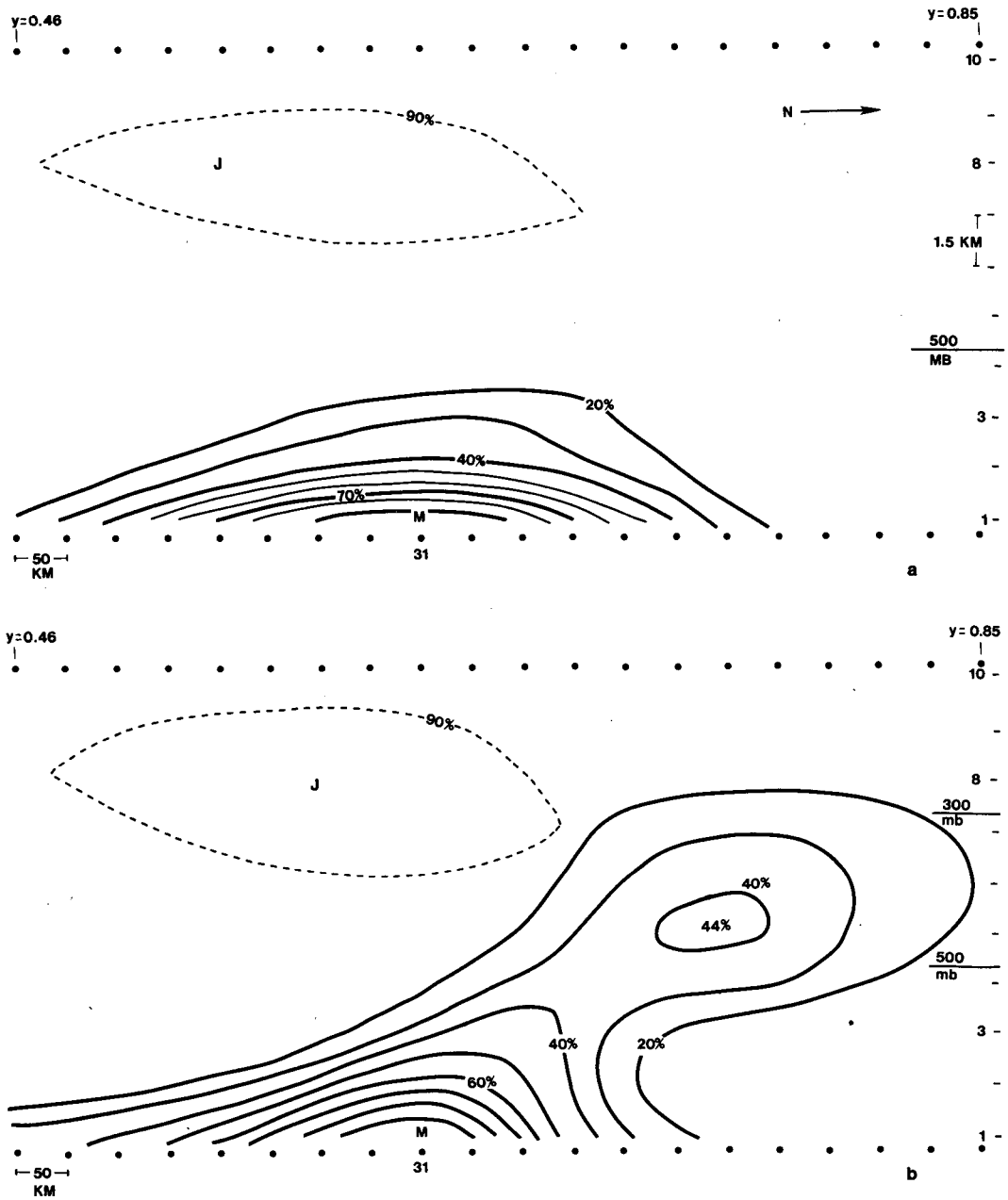

FIG. 2. Nondimensional disturbance amplitude $(\overline{p'^2})^{1/2}$ for fine resolution PE run. Portion of channel for $0.46 \leqq y \leqq 0.85$, $0 \leqq z \leqq 1$ is shown. Solid isolines are percent of maximum value at M. J locates jet core; dashed isotach is 90% of speed at J. Location of y grid points and k levels, as well as approximate location of 500 and 300 mb levels are shown. Panel a: Day 0; $M = 8.7 \times 10^{-4}$. Pattern is virtually the same as linear results. Panel b: Day 1; $M = 2.9 \times 10^{-3}$.

Our purpose here, however, is to see how much realism can be obtained through the use of completely dry models. There are (at least) three possible ways to proceed retaining a dry model. We can increase the realism of the linear model, we can increase the realism of the basic state or we can introduce nonlinear effects.

A recent example using the first two approaches is provided by a paper by Kent, Moore and Peltier (1987). They use a dry, semigeostrophic, linear model to study the instability of frontal zones, modeled by a Hoskins and Bretherton (1972) type front. While the basic state remains zonally independent, it possesses the asymmetric structure of wind and temperature in realistic frontal zones. Their basic-state front is wide and weak enough so that they argue it can be considered as a broad baroclinic zone and thus their results apply to PL/CC formation as well as to cyclone formation on a front. They obtain maximum growth rates for wave-

lengths ~1000 km; these disturbances grow via baroclinic instability. The growth rates for these disturbances are, however, 5–10 times smaller than either the observed PL/CC cases discussed by Sardie and Warner (1983) or our results shown in Fig. 1. Their disturbances, like ours, are quite shallow. Thus, while their study did not produce rapidly growing, deep disturbances, it shows that progress may be made by using non-QG linear models.

It is also interesting to note that their basic state did *not* include a layer of reduced stability in the lower troposphere. Inclusion of this effect would strengthen their argument that the results are applicable to PL/CC formation; our results suggest that enhanced growth rates would be produced.

The second approach mentioned above concerned increasing the realism of the basic state. This can also be done by relaxing the restriction of zonal independence. Reed (1979) pointed out that the use of a zonally independent basic state is probably not sufficiently realistic so the possibility exists that the linear results could be improved by using a nonzonally independent basic state simulating a long-wave trough within which PL/CC could develop. (Observed development within cyclonic flow regions is discussed in the next section.)

Other research suggests that this approach would bear fruit. Niehaus (1980, 1981) examined the instability of a nonzonal Eady problem, using a spectral technique and a multiple-scaling approach. Her results suggest that significant differences in disturbance amplitude would occur depending upon the location within a larger-scale wave. Maximum amplitudes occur downstream from the location of the maximum basic state temperature gradient, which is downstream from the "long wave" trough.

Another approach is that of Frederiksen (1979a) who used a two-layer, linear QG model on a sphere to study the growth of baroclinic disturbances within a planetary-scale wave. He found preferred regions for maximum intensity of the upper-level disturbance streamfunction to be downstream of the long wave troughs, on the cyclonic side of the long wave. Increasing the vertical resolution with a five-level model, he found similar results (Frederiksen, 1979b).

While the work cited here is for baroclinic waves on scales much larger than that of the phenomenon of interest to us, evidence does exist that use of a more realistic basic state within a dry, linear model will lead to more realistic simulations of PL/CC, in particular, a deeper vertical structure for disturbances evolving near the long wave trough.

To add a more realistic basic state in the above manner would introduce another dimension of complexity into this study, but a preliminary experiment was carried out along these lines using the PE model with surface friction. The same basic state as before was used, with the channel lengthened to 3600 km. The initial perturbation consisted of a 3600 km "long wave" plus three 1200 km "short waves." Both the long and short waves possessed the appropriate normal-mode structure, except that the structure of the long wave was modified by multiplying it by a function of height that reduced its initial amplitude to zero at the lowest two levels but left the amplitude unchanged at level 7 and above, with a linear change in between. The waves were aligned initially so that one of the short-wave troughs was situated in the long-wave trough. This modification to the long wave considerably reduced its initial growth rate.

The purpose of the experiment was to see if this short-wave trough would grow more rapidly than those not located near the long-wave trough. Thus the basic state plus the long wave were interpreted as the "new" basic state, with the short waves growing relative to this. Both long and short waves possessed small amplitudes initially so that the new basic state would change slowly and so that the short waves would approximate linear growth.

The results were in qualitative agreement with the work previously cited. The growth of the short waves was reviewed after 0.5 days when the disturbances were still small. After making allowances for some amplification of the long wave, the short wave located in the long-wave trough was stronger and possessed a greater amplitude at level $k = 5$, corresponding roughly to the 500 mb level, than did the short waves not in the long-wave trough. While this will be pursued further in future work, this experiment indicates that, with a dry model, PL/CC developing within a long-wave trough do in fact grow more rapidly and possess deeper structure than those developing in other locations.

Except for this preliminary experiment, increased realism of the basic state will not be attempted. Rather, we will retain the simplicity of the zonally independent basic state, but we will extend the realism of the solutions, including the deepening of the disturbance amplitude, by looking at nonlinear effects. This is discussed in the next section. Dry models combining both a more realistic basic state and nonlinear effects will remain the subject of future investigation.

5) The basic state zonal wind possesses a structure that can be both barotropically and baroclinically unstable. The 2DINIT results show that all modes with wavelengths greater than 1000 km grow by conversion of both zonal available potential energy and zonal kinetic energy to eddy energy, the former (baroclinic) process dominating for wavelengths below 2500 km. Below 1000 km waves grow only by the baroclinic process. Only for the "deep" disturbances with wavelengths of 3000 km or greater does the latter (barotropic) conversion process become nearly as important as the former. Thus, for wavelengths in the PL/CC range, barotropic instability is of little importance. These findings are in agreement with those of Sardie and Warner (1985, p 465).

To summarize this section, the linear analysis demonstrates that the addition of a region of reduced stability to the lowest 3 km of the basic state greatly am-

plifies the growth rates of disturbances possessing the dimensions of PL/CC. Thus, small-wavelength disturbances with rapid growth rates are produced by a dry, QG model. While no claim is made that moisture dynamics are unimportant, these results suggest that the initial stages of growth of PL/CC can be achieved without the inclusion of moisture effects. This is consistent with the observation of PL/CC-type phenomena over land (Mullen, 1982; Smart and Carr, 1986).

The short wavelength, linear disturbances are shallow. This discrepancy with some observed PL/CC will be reduced somewhat by the addition of nonlinear effects, as discussed in the next section.

5. The nonlinear results

Several integrations were carried out using the fully three-dimensional PE and QG models previously described. These runs went beyond the linear phase of growth, allowing the disturbance to achieve finite amplitude and to evolve through a life cycle. Parallel PE and QG nonfriction, coarse resolution runs were first made with Δx, $\Delta y = 100$ km. The channel length and width were 1200 and 3600 km, respectively. A PE run with surface friction also was made[2]. The PE runs were the extensions of the linear phase runs discussed in section 4. Based upon the outcome of these runs to 5.6 days, a fine-resolution run was made to three days using the PE model with friction. The channel width was reduced to 2400 km with Δx, $\Delta y = 50$ km for this run. All runs had ten vertical levels with $\Delta z = 1.5$ km.

For these runs, the linear, normal-mode solution was superimposed onto the basic state using an initially small amplitude. (5% of the maximum zonal wind U was used for the maximum value of the N–S component perturbation wind. Section 3b outlines the procedure used.) This superposition results in a level 1 pressure pattern at $t = 0$ with a small wave but no closed contours. The amplitude of this wave is 2.8 mb. Likewise, a small wave is present in the $t = 0$, level 1 buoyancy pattern. The units needed to dimensionalize p and b are found in Mudrick (1974, p 870), and the results displayed in the figures are surface pressure and temperature (in mb and degrees C, respectively).

The reasons for using a channel length, and hence a disturbance wavelength of 1200 km will now be discussed, followed by a description of the results. As discussed in section 4, no wavelength of maximum instability was found in the linear study. Thus a decision as to what disturbance wavelength to use had to be based upon other considerations. Atlantic polar low climatology studies and studies of North Pacific comma clouds often show the surface vortex to be located near a long-wave trough or a cyclonic vortex in the midtroposphere (the southern edge of the Aleutian low in the Pacific). Examples of such studies include Reed (1979), Locatelli et al. (1982), Businger (1985), Forbes and Lottes (1985, p 144) and Wilhelmsen (1985). It may also be that short waves or upper-level vortices within this larger-scale midtropospheric pattern often initiate surface development. Matsumoto et al. (1982, pp 342–343) show this occurring for a cold vortex aloft in the Western Pacific, behind the polar front, for example. The case presented by Wallace and Hobbs (1977, pp. 112 and 122) shows a short wave within the 500 mb flow; another over-land case with short waves at 500 mb is discussed by Smart and Carr (1986). Rasmussen (1985) describes an Atlantic polar low that develops from an upper-level cold core vortex. Thus, it may not be unreasonable to expect the horizontal size, i.e., wavelength of the developing surface feature to be "forced" to some extent by the finite-amplitude midtroposphere pattern, rather than to correspond to some wavelength of maximum instability for a zonally independent basic state.

Why 1200 km? Studies by Reed (1979) and by Locatelli et al. (1982) show 1000–1500 km to be typical spacings of Pacific comma cloud disturbances. Mullen's (1982) North America study had 1800 km as the spacing between such features, while Smart and Carr's (1986) case had a spacing of ~1000 km between vorticity maxima at 500 mb. Harrold and Browning (1969) found spacings of ~900 km for features they studied in the North Atlantic. It is seen that 1200 km falls within this spectrum of values. As will be discussed, the 1200 km fine-resolution run produced a low on the order of 500 km across, similar to the size of observed PL/CC pressure pattern disturbances, e.g., Locatelli et al. (1982, Fig. 13) and Rasmussen (1985, Fig. 7).

There were other reasons for using 1200 km. As the channel length is decreased, the linear disturbance structure becomes more shallow. This suggests that with a fixed Δz of 1.5 km (i.e., ten vertical levels), errors due to the limited vertical resolution should become larger as the channel length is reduced. Even for 1200 km the linear disturbance is quite shallow (Fig. 2a). A further decrease could exacerbate this potential problem, which was discussed in section 4. Finally, 1200 km was convenient from geometrical considerations (channel widths of 3600 and 2400 km were used) and from considerations of horizontal resolution, as well as finances.

An examination of the nonlinear results shows that the realism of the evolving disturbance is increased in several ways, compared to the linear results, "realism" being determined by features associated with observed PL/CC disturbances:

The disturbance has a life cycle lasting several days. The eddy kinetic energy (EKE) grows rapidly at first,

[2] Based on the runs with the "full friction" PE model discussed in section 4, use of the "full friction" PE model probably would not appreciably change the results presented in this section.

the linear growth phase lasting for ⅓ day or so. The EKE reaches a maximum for the PE runs at about day 1.2 (1.8 for the QG run); a relative minimum is reached between days 2½ and 3, depending on the particular run. The QG model energetics show the growth to be consistent with the baroclinic instability process, followed by barotropic damping as the EKE decreases toward the end of the cycle. For the PE fine-resolution run, the surface, central pressure deepens 7 mb by day 1½, compared to the surrounding pressure; thereafter slow filling occurs. Forbes and Lottes (1985) decided a pressure deficit of ~6 mb was needed to call observed disturbances "polar lows," so by their criteria our disturbance qualifies.

Disturbance amplitude increases in the midtroposphere due to nonlinear PE effects. Figure 2a presents the zonally averaged disturbance amplitude $(\overline{p'^2})^{1/2}$, where p' is the pressure deviation for day 0 for the fine-resolution run. The flow is out of the paper, the jet core is at J and the "90%" isotach for the zonally averaged wind is shown. A portion of the N–S (nondimensional) channel domain is shown for $0.46 \leqslant y \leqslant 0.85$ (the S and N walls are at $y = 0$ and 1, respectively) and for $0 \leqslant z \leqslant 1$. Maximum disturbance amplitude is at the bottom level $k = 1$ and the disturbance is seen to be quite shallow, the amplitude having fallen off to about 30% by level $k = 3$. Figure 2a is very similar to the linear results, and it displays the general shape of the QG disturbance structure over the lifetime of the coarse-resolution nonlinear run. Figure 2b displays the same result for day 1 for the PE fine-resolution run. Deepening of the disturbance has occurred at midtropospheric levels (the location of 500 and 300 mb is shown relative to the vertical scale). Since Fig. 2a shows the relative shape of the QG nonlinear results for day 1, the midtropospheric amplification seen in Fig. 2b must be due to nonlinear, nonquasi-geostrophic effects. While the PE disturbance at day 1 is still seen to be primarily a shallow feature, some midtropospheric amplification has occurred.

The extent of this midlevel amplification should not be overemphasized. An examination of the day 1 pressure pattern for $k = 5$, corresponding roughly to the 500 mb level, shows only a little change from the initial pattern. (These figures are not presented.) Thus this midlevel amplification is weak.

It is possible that this secondary maximum at midlevels seen in Fig. 2b represents the excitation of an internal mode rather than the upward extension of the initially shallow disturbance. The linear and nonlinear QG models allow for barotropic as well as for baroclinic instability, as do the PE models; since the secondary maximum is not observed in the QG models it seems logical that it is not associated with a barotropic or baroclinic instability of any type. A comparison of the nonlinear PE coarse-resolution surface friction and nonfriction runs shows the secondary maximum to be present in both; this suggests that surface friction is not responsible for the excitation of the secondary maximum. Apparently effects not associated with friction and not present in the QG models are responsible for the secondary maximum. If it represents some inertia–gravity wave mode not found in the QG models, it must behave strangely, since it forms quickly and maintains itself over the lifetime of the low-level disturbance. While the excitation of a secondary, internal mode cannot be ruled out as the reason for the secondary maximum in Fig. 2b, examination of the vertical motion and of the zonally averaged momentum flux (neither of which are shown) and the fact that the secondary maximum moves upward with time suggests it is an upward extension of the shallow initial disturbance.

Appearance of the surface "high"- and "low"-pressure regions becomes more realistic, as does the cold versus warm frontal configuration. Figure 3 presents dimensionalized output from the fine-resolution PE run for the lowest level $k = 1$, for pressure and temperature (derived from p and b, respectively).[3] By day ½ (Fig. 3a) a closed "low" has formed with a short "warm front," a region of enhanced temperature gradient extending to the southeast of the low. No "cold front" has yet appeared. By day ¾ (not shown), a cold front has appeared and by day 1 (Fig. 3b) an elongated cold front has formed south of the low, which has deepened by 3 mb in 12 hours. The leading edge of the cold front lies in the pressure trough extending south of the low. The warm front has remained as a short region extending just to the southeast of the low. A wider, weaker region of temperature change extends further southeast of the warm front. After this time the surface pressure pattern and position of the fronts remain about the same. Figure 5a shows this schematically.

Further details of the elongated cold front versus the short warm front can be deduced from Fig. 4. The relative vorticity at level 1 ($\frac{1}{2}\Delta z$ above the channel bottom, same as p and b), in units of $f_0 = 1.25 \times 10^{-4}$ s^{-1}, and the vertical motion w at level 1 (Δz or 1.5 km above the channel bottom), in units of cm s^{-1}, are shown for day 1, for the region within the rectangle shown in Fig. 3b. Note that using Δx, $\Delta y = 50$ km has allowed the intensity of the relative vorticity to obtain values greater than f_0 along the leading edge of the cold front and up to $4f_0$ near the low center, as well as allowing w to reach 16 cm s^{-1} ahead of the cold front and over 20 cm s^{-1} to the east of the low center on the northern edge of the short warm front. These frontal-scale intensities are quite respectable compared to the usually much weaker features produced by the PE model with a grid spacing on the order of 100 km. The

[3] There is a 9 mb difference N–S across the channel due to level $k = 1$ being $\frac{1}{2}\Delta z$, or 0.75 km above the channel bottom. Thus the basic state U is not zero at level 1. See Mudrick (1974, Fig. 2a) for a similar situation.

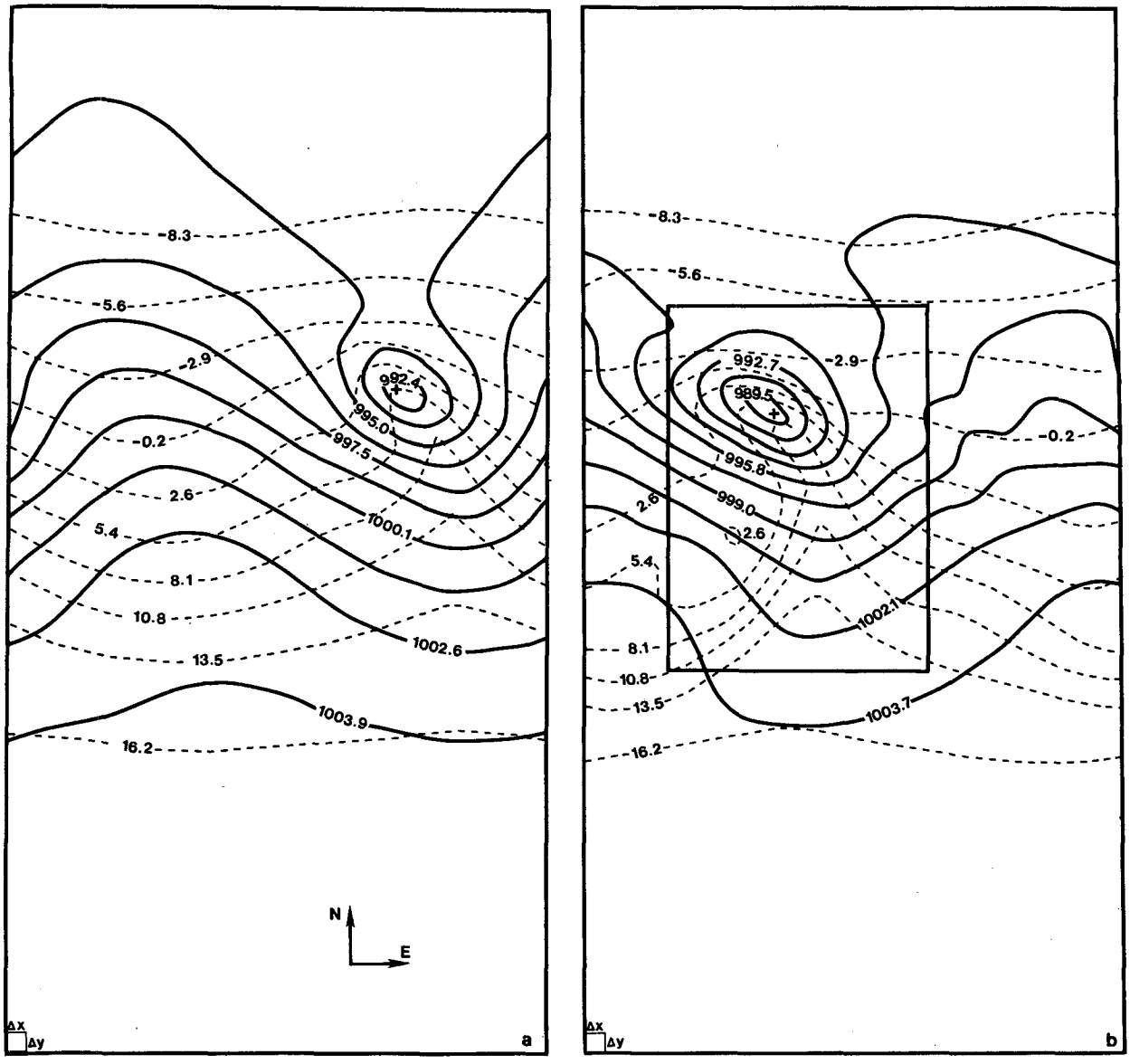

FIG. 3. Fine-resolution PE run, dimensional pressure (solid, mb) and temperature (buoyancy) (dashed, °C) for level $k = 1$. Grid square shown in SW corner. Panel a: Day ½; Min $p = 991.8$ mb. Panel b: Day 1; Min $p = 988.7$ mb. See text for details.

rapid appearance of the cold front within a 12-h period is also remarkable.

The day 1 nonlinear results (Fig. 3b) portray, along with the frontal zones, a small, fairly tight "low" on the order of 10 gridpoints or 500 km across. Associated with this is a broad, weak ridge but no closed contour "high". These features—the small "low", absence of a similar scale "high", the long cold front lying in a pressure trough with a quite short warm front—are all similar to synoptic analyses of disturbances associated with North Pacific comma clouds (Locatelli et al., 1982, Fig. 13). Atlantic polar low analyses also show the small vortex ~500 km across and an absence of similar scale "highs" (e.g., Rasmussen, 1985, Fig. 7). These features developed in this 1200 km run can also be contrasted to the features developed in other model integrations using the same model which simulated midlatitude, synoptic-scale cyclone waves. The latter cases possessed no layer of reduced stability and had channel lengths of 3000 to 5000 km. Figures 3, 4 and 10E and F in Mudrick (1974) typify such results; they show 1) a strong "high" as well as a large "low" which dominates the channel, and 2) a strong elongated warm front as well as a cold front. The 1200 km results are seen to be more similar to the PL/CC features than are the larger-scale results produced by the same model. There

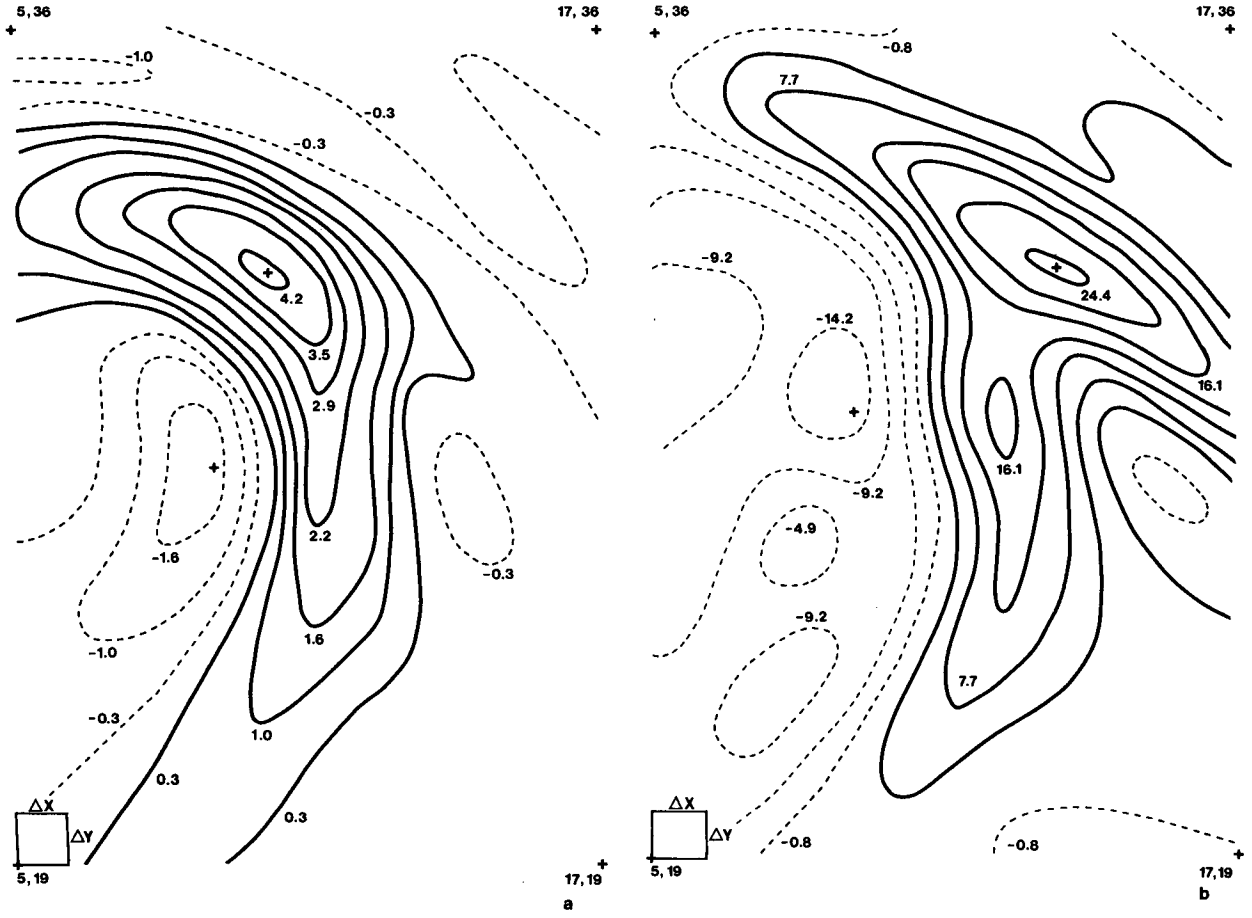

FIG. 4. Data from interior rectangle in Fig. 3b bounded by gridpoints shown. Negative isolines are dashed; $k = 1$. Panel a: relative vorticity $v_x - u_y$ in units of $f_0 = 1.25 \times 10^{-4}$ s^{-1}; Max = $4.5 f_0$, Min = $-1.9 f_0$. Panel b: Vertical motion w, cm s^{-1}; Max = 26.5 cm s^{-1}; Min = -15.4 cm s^{-1}.

are other realistic features of the 1200 km fine-resolution simulation: the low center lies under the cyclonic or cold side of the jet and the disturbance propagates eastward rapidly at $\sim$18 m s^{-1} in this case.

Aspects of an in situ occlusion can be seen. Little detailed analysis of frontal structure within observed PL/CC have been presented, due to lack of data. Locatelli et al. (1982, Fig. 19) present a schematic of a vortex with cold and occluded fronts; this is based in part on their Fig. 13. Their Fig. 19 shows a single occluded front extending from the vortex center, and beyond some point this is analyzed as a cold front.

An alternative interpretation of our Figs. 3a and 3b could be that shown in Fig. 5b: the region to the immediate southeast of the low center at day 1 is an occluded front, with the maximum temperature tongue extending southeast from the low, in the middle of the occluded front. Thus the northern end of the cold front and the short warm front are reinterpreted as a short occluded front. South and southwest of this region is the cold front. A very short warm frontal region could also be present. This interpretation is consistent with Fig. 19 from Locatelli et al. (1982). This alternative explanation is also consistent with Figs. 4a and 4b presented here since the tongue of maximum temperature, the line of maximum relative vorticity and the line of maximum cyclonic isobar curvature all lie within one grid distance of each other. Beyond day 1 the orientation of the frontal regions changes little; this is also consistent with the formation and maintenance of the "in situ" occlusion. Due to the shallowness of the disturbance and frontal zones, vertical cross sections do not shed any light on the "cold–warm" versus "occluded" interpretations.

Whether or not one interprets the frontal configuration as in Fig. 5a or as in Fig. 5b, we see that both on the disturbance scale and on the frontal scale, the nonlinear results have increased the realism of the simulation with respect to observed features of PL/CC.

6. Discussion and summary

As discussed previously, most PL/CC probably form beneath a region of cyclonic flow. Thus our results us-

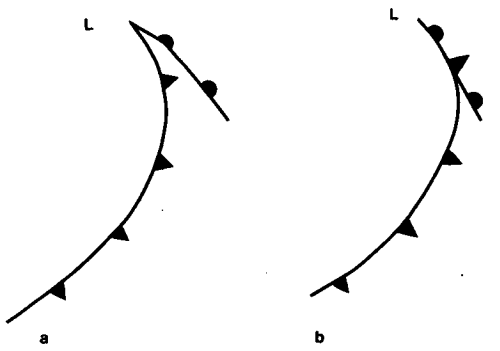

FIG. 5. Alternative interpretations of frontal configuration for Figs. 3b and 4. *L* marks lowest pressure. Panel a: Elongated cold front, short warm front. Panel b: Elongated cold front with short occluded region and possible warm front extension.

ing a zonally independent basic state might be expected to underestimate any development at midlevels. Nevertheless the nonlinear PE results show a deepening of the disturbance at midlevels, compared to the linear results, albeit the mature disturbance still is predominantly a shallow one. Dry, nonlinear models using more realistic basic states, i.e., those possessing midtropospheric waves, might be expected to produce even more realistic results as discussed in section 4. Preliminary work along these lines was described there; a short wave representing a PL/CC located within a long wave trough grew faster and obtained more amplitude at midlevels than did short waves not located near the trough. Further research in this direction is desirable.

The model results discussed here included implicitly the effect of surface fluxes of sensible heat by the inclusion of the layer of reduced stability. They have *not* included the effects of either stable or convective moisture processes (e.g., CISK). Studies such as Sardie and Warner (1983, 1985) have shown that inclusion of moisture dynamics enhances PL/CC development at midtropospheric levels. Likewise, the two-dimensional study of Orlanski (1986) shows the inclusion of regions of localized surface heating, such as warmer Gulf Stream water, leads to enhanced development of disturbances propagating across such regions.

Thus, as expected, the more physical effects that are included in simulation models, the more realistic will be the results. The purpose of this study, however, is to stress the amount of realism that can be achieved in simulating PL/CC disturbances with a model devoid of moisture dynamics, with the use of a very idealized basic state, and with only implicit surface heat fluxes. The linear, QG, frictionless study shows that shallow, subsynoptic-scale features with quite large growth rates result from the inclusion of the layer of reduced stability in the lower troposphere. The nonlinear PE results with friction show that, given sufficient horizontal resolution, these disturbances appear similar to observed PL/CC. This realism extends to the frontal scale, as deduced from comma cloud analyses presented by Locatelli et al. (1982). That such subsynoptic-scale features can occur in nature without significant moisture effects has been shown by the overland studies of Wallace and Hobbs (1977), Mullen (1982) and Smart and Carr (1986)[4].

Thus this work supports the statement by Orlanski (1986), previously quoted, that the dry atmosphere already has the necessary ingredients for the formation of subsynoptic-scale vortices and that the deepening is enhanced by the inclusion of moisture. Similar results were demonstrated by Sardie and Warner (1985), who present forecasting results for a comma cloud formation and a polar low situation using the "state of the art" Pennsylvania State University/National Center for Atmospheric Research mesoscale model. Their forecasts, while quite impressive, still show that significant errors in intensity and location of the disturbance exist for a 48-h forecast (e.g. their Figs. 2c and 6). Their model run without latent heating feedbacks (their Fig. 12a) shows development of a weaker polar low but at about the same location as in the moisture run.

Perhaps these results, taken together, suggest that accurate initial conditions of wind and temperature (as well as water vapor) are as important for the accurate forecasting of these subsynoptic-scale disturbances as is the inclusion of detailed moisture dynamics and simulation of the CISK process.

Acknowledgments. Part of this work was supported by NASA Grant NAG-5-381 and part by the University of Missouri—Columbia Agricultural Experiment Station Grant MO-00315. Much of the work described herein was completed while the author was on sabbatical leave at the Department of Atmospheric Science, State University of New York at Albany. The Department Chairman at SUNYA, Dr. Richard Orville, graciously provided computer funds as well as a terminal. The paper was typed by Betty Crowley. In addition, the aid of many people, both at UMC and SUNYA, was invaluable in seeing this work through to its completion. The aid of an anonymous reviewer is also appreciated.

APPENDIX

The Full-Friction PE Model

In order to add the effect of subgrid-scale turbulence to the PE model, in conjunction with the use of a layer of reduced stability (LRS) in the lowest 3 km, vertical stress terms were added to the momentum equations,

[4] The overland cases mentioned here may not have formed in a manner completely analogous to the mechanism presented here. Mullen (1982) presents a cross section showing a low-level stable layer as opposed to our low-level reduced stability, yet due to strong low-level vertical wind shear his case, like ours, possesses small Richardson numbers near the surface.

along with the surface stress. These terms were of the form $\partial\tau_x/\partial z$ where $\tau_x = A(z)\partial u/\partial z$, similarly for the y component. In finite differences, $\partial\tau_x/\partial z$ becomes $(1/\Delta z)(\tau_k - \tau_{k-1})$ where $\tau_k = (A_k/\Delta z)(u_{k+1} - u_k)$. τ_0 corresponds to the surface stress formulation (see section 2). Given the vertical resolution of the model ($\Delta z = 1.5$ km; adjacent A_ks are spaced that far apart), A_1 and A_2 represent values within the LRS while A_ks for $k \geq 3$ are above this region. Nondimensional values of A_1 and A_2 were chosen to correspond to a mean coefficient of eddy viscosity of 27 kg m^{-1} s^{-1} (270 gm cm^{-1} s^{-1}), a value presented by Palmen (1955). This value is for near-surface level winds; to use it for A_1 and A_2, i.e., over a depth of 3 km, may overestimate the turbulent mixing. For values above the LRS, the A_ks, for $k \geq 3$, were set equal to 10% of the value of A_1 and A_2; A_{10} was set to zero.

REFERENCES

Blumen, W., 1979: On short-wave baroclinic instability. *J. Atmos. Sci.*, **36,** 1925–1933.

——, 1980: On the evolution and interaction of short and long baroclinic waves of the Eady type. *J. Atmos. Sci.*, **37,** 1984–1993.

Businger, S., 1985: The synoptic climatology of polar low outbreaks. *Tellus,* **37A,** 419–432.

Duncan, C. N., 1977: A numerical investigation of polar lows. *Quart. J. Roy. Meteor. Soc.*, **103,** 255–267.

Forbes, G. S., and W. D. Lottes, 1985: Classification of mesoscale vortices in polar airstreams and the influence of the large-scale environment on their evolutions. *Tellus,* **37A,** 132–155.

Frederiksen, J. S., 1979a: The effects of long planetary waves on the regions of cyclogenesis: Linear theory. *J. Atmos. Sci.*, **36,** 195–204.

——, 1979b: Baroclinic instability of zonal flows and planetary waves in multi-level models on a sphere. *J. Atmos. Sci.*, **36,** 2320–2335.

Gall, R., 1976: The effects of released latent heat in growing baroclinic waves. *J. Atmos. Sci.*, **33,** 1686–1701.

Harrold, T. W., and K. A. Browning, 1969: The polar low as a baroclinic disturbance. *Quart. J. Roy. Meteor. Soc.*, **95,** 710–723.

Hoskins, B. J., and F. P. Bretherton, 1972: Atmospheric frontogenesis models: Mathematical formulation and solutions. *J. Atmos. Sci.*, **29,** 11–37.

James, I. N., and B. J. Hoskins, 1985: Some comparisons of atmospheric internal and boundary baroclinic instability. *J. Atmos. Sci.*, **42,** 2142–2155.

Kent Moore, G. W., and W. R. Peltier, 1986: Cyclogenesis in frontal zones. *J. Atmos. Sci.*, (in press.)

Locatelli, J. D., P. V. Hobbs and J. A. Werth, 1982: Mesoscale structures of vortices in polar air streams. *Mon. Wea. Rev.*, **110,** 1417–1433.

Mansfield, D. A., 1974: Polar lows: The development of baroclinic disturbances in cold air outbreaks. *Quart. J. Roy. Meteor. Soc.*, **100,** 541–554.

Matsumoto, S., K. Ninomiya, R. Hasegawa and Y. Miki, 1982: The structure and the role of a subsynoptic-scale cold vortex on the heavy precipitation. *Quart. J. Roy. Meteor. Soc. Japan,* **60,** 339–353.

Mudrick, S. E., 1974: A numerical study of frontogenesis. *J. Atmos. Sci.*, **31,** 869–892.

——, 1979: On the instability of asymmetric jets. *J. Atmos. Sci.*, **36,** 1217–1225.

——, 1982: A study of the adequacy of quasi-geostrophic dynamics for modeling the effect of cyclone waves on the larger scale flow. *J. Atmos. Sci.*, **39,** 2414–2430.

Mullen, S. L., 1979: An investigation of small synoptic-scale cyclones in polar air streams. *Mon. Wea. Rev.*, **107,** 1636–1647.

——, 1982: Cyclone development in polar air streams over the wintertime continent. *Mon. Wea. Rev.*, **110,** 1664–1676.

Niehaus, M. C. W., 1980: Instability of nonzonal baroclinic flows. *J. Atmos. Sci.*, **37,** 1447–1463.

——, 1981: Instability of nonzonal baroclinic flows: Multiple-scale analysis. *J. Atmos. Sci.*, **38,** 974–987.

Orlanski, I., 1986: Localized baroclinicity: A source for meso-α cyclones. *J. Atmos. Sci.*, **43,** 2857–2885.

Palmen, E., 1955: On the mean meridional drift of the frictional layer of the west wind belts. *Quart. J. Roy. Meteor. Soc.*, **81,** 459–461.

Rasmussen, E., 1983: A review of meso-scale disturbances in cold air masses. *Mesoscale Meteorology—Theories, Observations and Models,* D. K. Lilly and T. Gal-Chen, Eds., D. Reidel, 247–283.

——, 1985: A case study of a polar low development over the Barents Sea. *Tellus,* **37A,** 407–418.

Reed, R. J., 1979: Cyclogenesis in polar air streams. *Mon. Wea. Rev.*, **107,** 38–52.

Sanders, F., and J. R. Gyakum, 1980: Synoptic-dynamic climatology of the "Bomb." *Mon. Wea. Rev.*, **108,** 1589–1606.

Sardie, J. M., 1985: A numerical study of the development mechanisms of polar lows. *Tellus,* **37A,** 460–477.

——, and T. T. Warner, 1983: On the mechanism for the development of polar lows. *J. Atmos. Sci.*, **40,** 869–881.

Smart, J. R., and F. H. Carr, 1986: Observations and analysis of a polar low over the Great Lakes region. *Proc., Eleventh Conf. on Weather Forecasting and Analysis, Kansas City,* Amer. Meteor. Soc., 188–193.

Staley, D. O., and R. L. Gall, 1977: On the wavelength of maximum baroclinic instability. *J. Atmos. Sci.*, **34,** 1679–1688.

——, T. C. Adang and L. M. Maier, 1987: Baroclinic instability in a model with shear and static stability adjustable in the meridional plane. *J. Atmos. Sci.*, **44,** 2097–2119.

Wallace, J. M., and P. V. Hobbs, 1977: *Atmospheric Science: an Introductory Survey.* Academic Press, 467 pp.

Wilhelmsen, K., 1985: Climatological study of gale-producing polar lows near Norway. *Tellus,* **37A,** 451–459.